Spin filter effect of manganese phthalocyanine contacted with single-walled carbon nanotube electrodes

Xin Shen,[1] Lili Sun,[1] Enrico Benassi,[2] Ziyong Shen,[1] Xingyu Zhao,[1] Stefano Sanvito,[3] and Shimin Hou[1,a)]

[1]*Department of Electronics, Key Laboratory for the Physics and Chemistry of Nanodevices, Peking University, Beijing 100871, China*
[2]*Department of Chemistry, Division of Physical Chemistry, University of Modena and Reggio Emilia, 41100 Modena, Italy and Center for Organic Electronics and Photonics, School of Chemistry and Biochemistry, Georgia Institute of Technology, Atlanta, Georgia 30332, USA*
[3]*School of Physics and CRANN, Trinity College, Dublin 2, Ireland*

(Received 19 October 2009; accepted 11 January 2010; published online 1 February 2010)

We present a theoretical study of the spin transport through a manganese phthalocyanine (MnPc) molecule sandwiched between two semi-infinite armchair single-walled carbon nanotube (SWCNT) electrodes. *Ab initio* modeling is performed by combing the nonequilibrium Green's function formalism with spin density functional theory. Our calculations show that MnPc not only can act as a nearly perfect spin filter, but also has a large transmission around the Fermi level, which is dominated by the highest occupied molecule orbital (HOMO). The HOMO of MnPc is found to be a singly filled doubly degenerate molecular orbital, where the electrodes' Fermi level can easily pin. The spin filter effect of MnPc is very robust regardless of whether the open ends of the SWCNT electrodes are terminated by hydrogen, fluorine, or carbon dimers, demonstrating its promising applications in future molecular spintronics. © *2010 American Institute of Physics*.
[doi:10.1063/1.3302258]

I. INTRODUCTION

Molecular spintronics, in which molecules are used as spin transport channels, has the potential of becoming a viable way for controlling and manipulating the quantum transport properties of spins at the single-molecule level.[1–4] Among the many potential molecular candidates,[5–12] metal (II) phthalocyanines (MPc) form a promising and important family of compounds whose spin states can be systematically altered by changing the metal center atom.[13] At present, many experimental and theoretical investigations have focused on electronic properties of MPc molecules adsorbed on metal substrates,[14–19] among which manganese phthalocyanine (MnPc) is a representative.[16,17] However, a few studies on the electronic transport properties of MPc in the lead-molecule-lead configuration have been reported, especially for MPc molecules sandwiched between low-dimensional electrodes.[20–22] Note that low-dimensional electrodes whose size is comparable to that of the molecules to be measured will be important for future integrated circuits based on molecular devices, because bulk contacts can only be used as electron source and sink.[23–25] Although preliminary results about a prototypical single-molecule device composed of a MnPc molecule between two one-dimensional gold monatomic chains have been reported previously,[22] it is extremely difficult to build such devices and then measure their transport properties because freely suspended gold monatomic chains created in current experiments are usually only two or three atoms long.[26]

In contrast to metallic monatomic chains, nearly perfect single-walled carbon nanotubes (SWCNTs), which are molecular objects themselves, can be routinely synthesized using the technique of arc discharge, laser ablation, or chemical vapor deposition.[27] More importantly, SWCNTs have been recently employed as the electrodes for molecular devices,[28–30] and preliminary experimental and theoretical results have shown that devices made with SWCNT electrodes can have better performance than those made with traditional metal electrodes.[31,32] Therefore, here we investigate the spin transport properties of a MnPc molecule sandwiched between two semi-infinite armchair SWCNT electrodes. This is realized by employing the nonequilibrium Green's function formalism combined with spin density functional theory (that is, the NEGF+DFT approach).[33–42] Our calculations show that MnPc can act as a nearly perfect spin filter and also has a large transmission around the Fermi level (E_F). The highest occupied molecular orbital (HOMO) of MnPc is a doubly degenerate state composed of the Mn $3d_{xz}$ or $3d_{yz}$ atomic orbitals. These are π-type orbitals delocalized along the entire molecule thus that they can couple with the conducting states of the SWCNT electrodes forming efficient conducting channels around the Fermi level.

II. CALCULATION METHOD

Geometry optimization and electronic structure calculations have been performed by using the SIESTA package.[43] We use improved Troullier–Martins pseudopotentials to describe the core electrons and the generalized gradient approximation (GGA) of Perdew, Burke, and Ernzerhof (PBE)

[a)]Author to whom correspondence should be addressed. Electronic mail: smhou@pku.edu.cn.

for the exchange and correlation energy.[44,45] The wave functions for the valence electrons are expanded over a finite range numerical basis set, and a user-defined double zeta plus polarization basis set is constructed for all elements including hydrogen, carbon, nitrogen, and manganese. Geometry optimization is obtained by conjugate gradient relaxation until the forces are smaller than 0.03 eV $Å^{-1}$. For comparison, all-electron DFT calculations for isolated MnPc molecules are also carried out using both the PBE GGA functional and the PBEh hybrid functional with the GAUSSIAN03 code.[46–48] Here, the 6-311++G(d,p) basis sets are used for carbon, hydrogen and nitrogen atoms,[49] and the cc-pVTZ basis set is used for the Mn ion.[50]

The spin-polarized transport calculations have been performed by using the SMEAGOL package,[39–41] which is a practical implementation of the NEGF+DFT approach. Since SMEAGOL uses SIESTA as the DFT platform, we employ the same pseudopotentials, basis set and GGA functional, for both the geometry relaxation and the transport. Considering the atomic and electronic structure of SWCNTs, two semi-infinite (4,4) armchair SWCNTs are chosen as the electrodes.[51] The charge density is integrated over 80 energy points along the semicircle, 25 energy points along the line in the complex plane and 20 poles in the Fermi distribution (the electronic temperature is 25 meV). The zero-bias transmission functions for the spin-up and spin-down electrons ($\sigma = \uparrow / \downarrow$) are calculated from the Landauer formula,

$$T_\sigma(E) = Tr[\Gamma_1 G_\sigma \Gamma_2 G_\sigma^+](E),$$

where G_σ is the spin-dependent retarded Green's function of the extended molecule and $\Gamma_{1,2}$ are the broadening functions of the left and right electrodes. It should be noted that the broadening functions $\Gamma_{1,2}$ are independent of spin since the semi-infinite SWCNT electrodes are not spin-polarized. More details about the numerical implementation can be found in the literature.[39–41]

III. RESULTS AND DISCUSSION

First we investigate the atomic and electronic structure of the isolated MnPc molecule. As shown in Fig. 1(a), MnPc is a planar molecule with D_{4h} symmetry, where the central Mn ion is surrounded by four isoindole groups bridged by four additional nitrogen atoms. On the basis of the electron counting rules for the Pc ligands, the central Mn ion has a 2+ formal charge. The optimized bond lengths of MnPc are listed in Table I. When compared with the corresponding experimental values,[52] all of the bond lengths calculated with SIESTA are slightly overestimated. This must be attributed to the PBE GGA functional, because the same trend is also observed in the all-electron DFT calculation with the same functional but a much larger basis set (the calculation is performed with GAUSSIAN03). In contrast, the deviations of the bond lengths calculated with the PBEh hybrid functional from the experimental values are a little reduced, which is a well-known behavior of these functionals for organic compounds.[53]

In the MnPc molecule, the strong crystalline field of D_{4h} symmetry splits the Mn $3d$ atomic orbitals into $a_{1g}(d_{z^2})$, $b_{2g}(d_{xy})$, $e_g(d_{xz},d_{yz})$, and $b_{1g}(d_{x^2-y^2})$. The most important and intriguing problem concerning with the electronic structure of MnPc is the determination of the energy position of these $3d$ orbitals with respect to the $a_{1u}(\pi)$ and $2e_g(\pi^*)$ orbitals, which are, respectively, the HOMO and the lowest unoccupied molecular orbital (LUMO) of the Pc ring. The energy diagram of these key molecular orbitals of MnPc is given in Fig. 1(b). As we can see, the ground state of the MnPc molecule is determined to be a quadruplet where the HOMO is a singly filled doubly degenerate state with the e_g symmetry

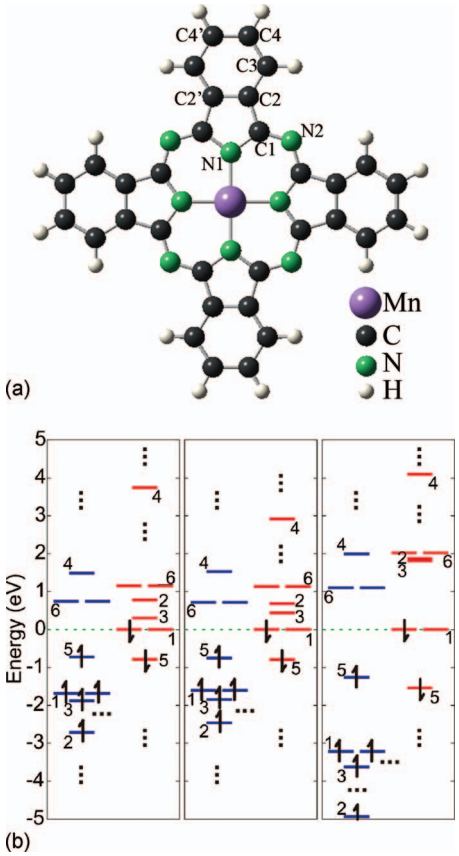

FIG. 1. Atomic and electronic structure of the isolated MnPc molecule with D_{4h} symmetry. In (a) optimized molecular structure. In (b) energy diagrams (left: PBE/SIESTA, middle: PBE/GAUSSIAN03, and right: PBEh/GAUSSIAN03) of selected frontier molecular orbitals, here orbitals 1–6 represent e_g, a_{1g}, b_{2g}, b_{1g}, a_{1u}, and $2e_g$, respectively.

TABLE I. Optimized bond lengths (in Å) of the MnPc molecule in the gas phase calculated with SIESTA and GAUSSIAN03. The experimental values are also given for comparison.

		GAUSSIAN03		
Bond	SIESTA	PBE	PBEh	Expt.[a]
Mn–N1	1.957	1.951	1.945	1.937
N1–C1	1.395	1.395	1.378	1.386
N2–C1	1.326	1.326	1.316	1.323
C1–C2	1.458	1.453	1.447	1.450
C2–C2′	1.417	1.412	1.400	1.392
C2–C3	1.406	1.401	1.392	1.396
C3–C4	1.403	1.398	1.387	1.380
C4–C4′	1.418	1.413	1.404	1.391

[a]Reference 52.

for the spin-down electrons. Using the same PBE functional, the energy levels obtained from the all-electron DFT calculation performed with GAUSSIAN03 are almost the same as those calculated with SIESTA, further confirming the appropriateness of the pseudopotentials and basis functions for the C, N, H, and Mn atoms built for this work.

Due to the strong electron correlation in the MPc molecules, it is instructive to discuss the influence of the choice of the DFT functional on the calculated MnPc electronic structure. Since a fraction of the exact (Fock) exchange is included in hybrid functionals, the self-interaction error is much mitigated when compared to that of the GGA functionals. Therefore, it has been argued that the hybrid functionals are much more appropriate to deal with MPc molecules than the GGA functionals.[54–56] For the MnPc molecule, the PBEh hybrid functional provides the same ground state electronic configuration as that of the PBE GGA functional, as shown in Fig. 1(b). However, the choice of the DFT functionals does affect the energy position of molecular orbitals: the separations among the energy levels obtained with the PBEh functional are larger than those obtained by employing PBE. Although the a_{1g} and b_{2g} orbitals of the spin-down electrons have also been calculated to be the HOMO of MnPc,[56] the HOMO with the e_g symmetry calculated using both the PBE and PBEh functionals here is more consistent with the most recent experimental electronic excitation spectrum of MnPc films.[57] In particular, by using the PBE GGA functional the energy gap between the HOMO (e_g) and the HOMO-1 (a_{1u}) of MnPc is calculated to be 0.78 and 0.79 eV, respectively, with SIESTA and GAUSSIAN03. This is much closer to the experimentally observed excitation of 0.5 eV than the value of 1.54 eV given by the PBEh hybrid functional. We then conclude that, at least for the MnPc molecule, the PBE GGA functional is a better choice than hybrid functionals such as PBEh.

Now we move to investigate the transport properties of MnPc sandwiched between two semi-infinite (4,4) armchair SWCNT electrodes, where dangling bonds at the open end of each SWCNT electrode are terminated with hydrogen atoms.[58] Figure 2(a) shows the optimized geometric structure of the SWCNT-MnPc-SWCNT junction. By construction, the (4,4) armchair SWCNT electrodes are placed along the x-axis, and the MnPc molecule is placed in the xOy plane. Due to the presence of two semi-infinite SWCNT electrodes, the symmetry of MnPc in the junction is reduced, losing its inversion center. For example, the Mn–N bond lengths are changed from 1.957 Å in the isolated molecule to 1.948 Å along the transport direction and 1.963 Å perpendicular to the transport direction, respectively.

We remark that the SWCNT-MnPc-SWCNT junction proposed here can be possibly synthesized in light of the idea that the growth of armchair SWCNTs along the axial direction can be realized by cycloaddition with alkyne.[59] For example, since SWCNTs have reactive ends to which a wide variety of species can be covalently attached,[60] a bis(dibromomethyl)-SWCNT complex can be obtained by adding two dibromomethyl groups to a carbon dimer at the open end. This gives a diene under catalyticaction. Then, a

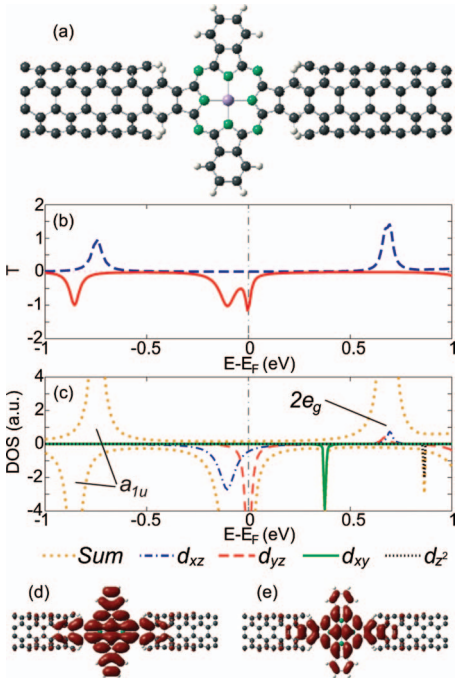

FIG. 2. Transport properties of MnPc coupled to two semi-infinite (4,4) armchair SWCNT electrodes, and dangling bonds at the open ends are terminated with hydrogen atoms. In (a) optimized geometrical structure of the SWCNT-MnPc-SWCNT junction. In (b) the energy-dependent spin-resolved transmission spectrum, the blue (dashed) and red (solid) curves are, respectively, for the spin-up and spin-down electrons. In (c) the DOS projected onto the central MnPc molecule. In [(d) and (e)] the isosurfaces of the two eigenchannels for the spin-down electrons calculated at the Fermi level and 0.10 eV below the Fermi level, respectively.

manganese dibenzoporphyrazine molecule can be connected to two dienes by the two newly formed six-membered rings through cycloaddition, leading to an SWCNT-MnPc-SWCNT junction.

Going now to the transport, in Fig. 2(b) we present the calculated spin-resolved transmission as a function of energy, $T(E)$, for the SWCNT-MnPc-SWCNT junction. As we can see, MnPc retains its spin polarization even after being contacted to the SWCNT electrodes. Around the Fermi level, the molecule exhibits a dual-peak transmission structure approaching unity for the spin-down electrons and a negligible transmission for the spin-up ones. In order to measure quantitatively the spin filtering efficiency, we define the transport spin polarization at the Fermi level as $[T_{\downarrow}(E_F)-T_{\uparrow}(E_F)]/T_{\downarrow}(E_F)$. Our calculations show that, when coupled to the (4,4) armchair SWCNT electrodes, MnPc exhibits nearly perfect spin filtering with a spin polarization approaching 100%. Therefore, at the PBE GGA level, MnPc not only can act as a nearly perfect spin filter but also has a large transmission around the Fermi level.

A deeper insight into the conductance of the SWCNT-MnPc-SWCNT junction can be obtained by projecting the density of states (DOS) of the junction onto the frontier molecular orbitals of the central MnPc molecule, which is shown in Fig. 2(c). This is realized by using our previously developed projection method based on scattering states.[61] For MnPc contacted to the (4,4) armchair SWCNT electrodes, the transmission peaks of the spin-down electrons

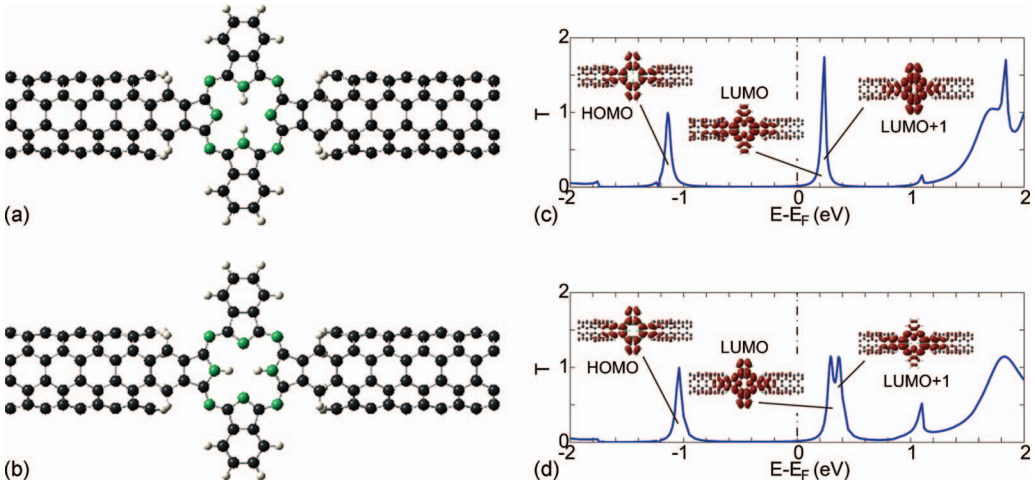

FIG. 3. Transport properties of H_2Pc coupled to two semi-infinite (4,4) armchair SWCNT electrodes, and dangling bonds at the open ends are terminated with hydrogen atoms. Optimized geometrical structures of the SWCNT-H_2Pc-SWCNT junctions where the two inner hydrogen atoms are along the transport direction (a) or perpendicular to the transport direction (b). In [(c) and (d)] the corresponding energy-dependent transmission spectra of the two junctions shown in (a) and (b), the inserts are the isosurfaces of the eigenchannels dominated by the HOMO, LUMO, and LUMO+1 orbitals of the H_2Pc molecule.

around E_F are mainly contributed by the HOMO of MnPc whose degeneracy is lifted in the junction due to the reduced symmetry. The lower and wide transmission peak corresponds to the Mn $3d_{xz}$ atomic orbital, due to the strong interaction with the SWCNT electrodes. In contrast, the upper and sharp transmission peak corresponds to the Mn $3d_{yz}$ atomic orbital, due to the relatively weak interaction with the SWCNT electrodes. This can be seen more clearly from the isosurfaces of the two eigenchannels calculated at the Fermi level and at 0.10 eV below E_F [see Figs. 2(d) and 2(e)]. Since the HOMO of MnPc is a π-type orbital delocalized along the entire molecule, the two broadened transmission peaks overlap onto each other, thus that the electrodes' Fermi level can pin at the HOMO, leading to a large transmission around E_F for the spin-down electrons. The a_{1u} orbital of the Pc ring forms two transmission peaks at 0.74 and 0.86 eV below the Fermi level for the spin-up and spin-down electrons, respectively. Finally the spin-up transmission peak at 0.70 eV above E_F is mainly formed by the $2e_g$ orbital of the Pc ring.

In order to demonstrate further the important role played by the Mn ion in the spin transport of the MnPc molecule, we investigate the conductance of metal-free phthalocyanine (H_2Pc) coupled to two semi-infinite (4,4) armchair SWCNT electrodes. Two different structures are possible for the SWCNT-H_2Pc-SWCNT junction due to the D_{2h} symmetry of the H_2Pc molecule: the first one has the two inner hydrogen atoms oriented along the transport direction, while in the second one the two inner hydrogen atoms are perpendicular to it. The optimized geometries and the corresponding transmission spectra of these two junctions are presented in Fig. 3. Without the Mn ion, the transmission curves of the two SWCNT-H_2Pc-SWCNT junctions are both spin-degenerate and have a negligibly small value around E_F because none of the transmission peaks contributed by the HOMO, LUMO, and LUMO+1 orbitals of the H_2Pc molecule cuts across the Fermi level. The striking difference between the two transmission spectra is the appearance of the transmission peaks dominated by the LUMO and LUMO+1 orbitals of the H_2Pc molecule. When the two inner hydrogen atoms are perpendicular to the transport direction, these two peaks merge into a single one; in contrast, when the two inner hydrogen atoms are along the transport direction, these two peaks can be discerned clearly.

Finally, we investigate whether or not the type of termination of the SWCNTs' open ends affects the spin transport of MnPc. The question is intriguing since some electronic properties such as field emission of open-ended SWCNTs depend critically on the way the ends are terminated. For this purpose, we consider two more termination configurations besides passivating the dangling bonds with hydrogen. The first one uses pristine (4,4) armchair SWCNT electrodes, in which carbon dimers are formed at the open end after relaxation.[58] In the second one, hydrogen is replaced by fluorine, which has a larger electronegativity. The calculated spin-resolved transmission spectra of the two new junctions are presented in Fig. 4. When compared with the hydrogen passivation, the termination of the open ends of the (4,4) armchair SWCNT electrodes with carbon dimers or fluorine atoms only affects marginally the overall shape of the transmission curve of the SWCNT-MnPc-SWCNT junction, espe-

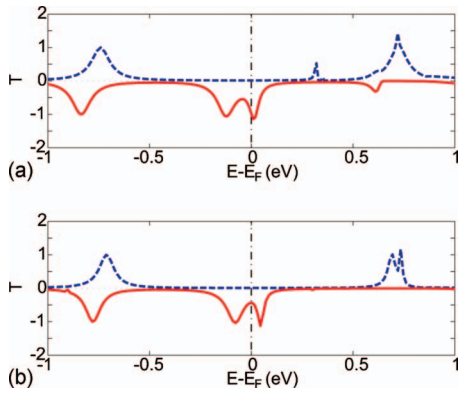

FIG. 4. The energy-dependent spin-resolved transmission spectra of the SWCNT-MnPc-SWCNT junctions with the open ends terminated by (a) pristine carbon dimers and (b) fluorine atoms. Here, the blue (dashed) and red (solid) curves are for the spin-up and spin-down electrons, respectively.

cially in the energy region around E_F. This demonstrates the robustness of the spin polarization of MnPc attached to armchair SWCNT electrodes. Our results however should not be surprising. Typically the local DOS at the open end and the work function of SWCNTs, thus their field emission properties are significantly affected by different termination atoms. However different chemical terminations cannot influence too much the coupling of the MnPc molecule to the (4,4) armchair SWCNT electrodes, because the chemical bonding between the MnPc molecule and the SWCNT electrodes is electronically localized and the distance between the termination atoms and the bonding site is far enough even for the (4,4) armchair SWCNT.

IV. CONCLUSION

We have investigated the atomic structure, electronic structure and spin transport properties of MnPc attached to two semi-infinite (4,4) armchair SWCNT electrodes. The ground state of MnPc in the gas phase is determined to be a quadruplet, and the HOMO is a singly filled doubly degenerate orbital with the e_g symmetry. Though the degeneracy of the HOMO is lifted in the SWCNT-MnPc-SWCNT junction due to the presence of the two SWCNT electrodes, MnPc still retains its spin polarization and the two broadened transmission peaks dominated by the HOMO overlap with each other thus that the electrodes' Fermi level can pin. Therefore, MnPc not only can act as a nearly perfect spin filter but also has a large transmission around the Fermi level. Furthermore we have found that the spin polarization of the SWCNT-MnPc-SWCNT junctions is very robust to the termination type of the open ends of the SWCNT electrodes. These junctions then appear as promising building blocks for future molecular spintronic devices.

ACKNOWLEDGMENTS

This project was supported by the National Natural Science Foundation of China (Grant No. 60771002), the Ministry of Education (Grant No. NCET-07-0014) and the MOST of China (Grant Nos. 2006CB932404 and 2007CB936204). The Smeagol project (SS) is supported by Science Foundation of Ireland.

[1] S. Sanvito, J. Mater. Chem. **17**, 4455 (2007).
[2] L. Bogani and W. Wernsdorfer, Nature Mater. **7**, 179 (2008).
[3] W. Y. Kim, Y. C. Choi, and K. S. Kim, J. Mater. Chem. **18**, 4510 (2008).
[4] W. Y. Kim, Y. C. Choi, and K. S. Kim, Acc. Chem. Res. **43**, 111 (2010).
[5] V. V. Maslyuk, A. Bagrets, V. Meded, A. Arnold, F. Evers, M. Brandbyge, T. Bredow, and I. Mertig, Phys. Rev. Lett. **97**, 097201 (2006).
[6] H. Xiang, J. Yang, J. G. Hou, and Q. Zhu, J. Am. Chem. Soc. **128**, 2310 (2006).
[7] M. Mannini, F. Pineider, P. Sainctavit, C. Danieli, E. Otero, C. Sciancalepore, A. M. Talarico, M. Arrio, A. Cornia, D. Gatteschi, and R. Sessoli, Nature Mater. **8**, 194 (2009).
[8] L. Zhou, S. W. Yang, M. F. Ng, M. B. Sullivan, V. B. C. Tan, and L. Shen, J. Am. Chem. Soc. **130**, 4023 (2008).
[9] X. Shen, Z. Yi, Z. Shen, X. Zhao, J. Wu, S. Hou, and S. Sanvito, Nanotechnology **20**, 385401 (2009).
[10] K. Xu, J. Huang, S. Lei, H. Su, F. Y. C. Boey, Q. Li, and J. Yang, J. Chem. Phys. **131**, 104704 (2009).
[11] C. D. Pemmaraju, I. Rungger, and S. Sanvito, Phys. Rev. B **80**, 104422 (2009).
[12] S. K. Shukla and S. Sanvito, Phys. Rev. B **80**, 184429 (2009).
[13] M.-S. Liao and S. Scheiner, J. Chem. Phys. **114**, 9780 (2001).
[14] A. Zhao, Q. Li, L. Chen, H. Xiang, W. Wang, S. Pan, B. Wang, X. Xiao, J. Yang, J. G. Hou, and Q. Zhu, Science **309**, 1542 (2005).
[15] L. Gao, W. Ji, Y. B. Hu, Z. H. Cheng, Z. T. Deng, Q. Liu, N. Jiang, X. Lin, W. Guo, S. X. Du, W. A. Hofer, X. C. Xie, and H.-J. Gao, Phys. Rev. Lett. **99**, 106402 (2007).
[16] Y.-S. Fu, S.-H. Ji, X. Chen, X.-C. Ma, R. Wu, C.-C. Wang, W.-H. Duan, X.-H. Qiu, B. Sun, P. Zhang, J.-F. Jia, and Q.-K. Xue, Phys. Rev. Lett. **99**, 256601 (2007).
[17] Z. Hu, B. Li, A. Zhao, J. Yang, and J. G. Hou, J. Phys. Chem. C **112**, 13651 (2008).
[18] X. Chen, Y.-S. Fu, S.-H. Ji, T. Zhang, P. Cheng, X.-C. Ma, X.-L. Zou, W.-H. Duan, J.-F. Jia, and Q.-K. Xue, Phys. Rev. Lett. **101**, 197208 (2008).
[19] S.-H. Chang, S. Kuck, J. Brede, L. Lichtenstein, G. Hoffmann, and R. Wiesendanger, Phys. Rev. B **78**, 233409 (2008).
[20] G. V. Nazin, X. H. Qiu, and W. Ho, Science **302**, 77 (2003).
[21] T. Tada, S. Hamayama, M. Kondo, and K. Yoshizawa, J. Phys. Chem. B **109**, 12443 (2005).
[22] A. Calzolari, A. Ferretti, and M. B. Nardelli, Nanotechnology **18**, 424013 (2007).
[23] W. Lu and C. M. Lieber, Nature Mater. **6**, 841 (2007).
[24] Z. Qian, R. Li, S. Hou, Z. Xue, and S. Sanvito, J. Chem. Phys. **127**, 194710 (2007).
[25] Z. Qian, R. Li, X. Zhao, S. Hou, and S. Sanvito, Phys. Rev. B **78**, 113301 (2008).
[26] W. H. A. Thijssen, D. Marjenburgh, R. H. Bremmer, and J. M. van Ruitenbeek, Phys. Rev. Lett. **96**, 026806 (2006).
[27] H. Dai, in *Nanotube Growth and Characterization, Carbon Nanotubes*, edited by M. S. Dresselhaus, G. Dresselhaus, and P. Avouris (Springer, Berlin, 2001).
[28] X. Guo, J. P. Small, J. E. Klare, Y. Wang, M. S. Purewal, I. W. Tam, B. H. Hong, R. Caldwell, L. Huang, S. O'Brien, J. Yan, R. Breslow, S. J. Wind, J. Hone, P. Kim, and C. Nuckolls, Science **311**, 356 (2006).
[29] X. Guo, A. A. Gorodetsky, J. Hone, J. K. Barton, and C. Nuckolls, Nat. Nanotechnol. **3**, 163 (2008).
[30] X. Guo, S. Xiao, M. Myers, Q. Miao, M. L. Steigerwald, and C. Nuckolls, Proc. Natl. Acad. Sci. U.S.A. **106**, 691 (2009).
[31] P. Qi, A. Javey, M. Rolandi, Q. Wang, E. Yenilmez, and H. Dai, J. Am. Chem. Soc. **126**, 11774 (2004).
[32] Y. Cho, W. Y. Kim, and K. S. Kim, J. Phys. Chem. A **113**, 4100 (2009).
[33] Y. Meir and N. S. Wingreen, Phys. Rev. Lett. **68**, 2512 (1992).
[34] P. Hohenberg and W. Kohn, Phys. Rev. **136**, B864 (1964).
[35] W. Kohn and L. J. Sham, Phys. Rev. **140**, A1133 (1965).
[36] J. Zhang, S. Hou, R. Li, Z. Qian, R. Han, Z. Shen, X. Zhao, and Z. Xue, Nanotechnology **16**, 3057 (2005).
[37] Y. Xue, S. Datta, and M. A. Ratner, Chem. Phys. **281**, 151 (2002).
[38] M. Brandbyge, J.-L. Mozos, P. Ordejón, J. Taylor, and K. Stokbro, Phys. Rev. B **65**, 165401 (2002).
[39] A. R. Rocha, V. M. García-Suárez, S. W. Bailey, C. J. Lambert, J. Ferrer, and S. Sanvito, Nature Mater. **4**, 335 (2005).
[40] A. R. Rocha, V. M. García-Suárez, S. Bailey, C. Lambert, J. Ferrer, and S. Sanvito, Phys. Rev. B **73**, 085414 (2006).
[41] I. Rungger and S. Sanvito, Phys. Rev. B **78**, 035407 (2008).
[42] W. Y. Kim and K. S. Kim, J. Comput. Chem. **29**, 1073 (2008).
[43] J. M. Soler, E. Artacho, J. D. Gale, A. García, J. Junquera, P. Ordejón, and D. Sánchez-Portal, J. Phys.: Condens. Matter **14**, 2745 (2002).
[44] N. Troullier and J. Martins, Phys. Rev. B **43**, 1993 (1991).
[45] J. Perdew, K. Burke, and M. Ernzerhof, Phys. Rev. Lett. **77**, 3865 (1996).
[46] J. Perdew, M. Ernzerhof, and K. Burke, J. Chem. Phys. **105**, 9982 (1996).
[47] M. Ernzerhof and G. E. Scuseria, J. Chem. Phys. **110**, 5029 (1999).
[48] M. J. Frisch, G. W. Trucks, H. B. Schlegel *et al.*, GAUSSIAN03, Revision C.02, Gaussian, Inc., Pittsburg PA, 2003.
[49] M. J. Frisch, J. A. Pople, and J. S. Binkley, J. Chem. Phys. **80**, 3265 (1984).
[50] N. B. Balabanov and K. A. Peterson, J. Chem. Phys. **123**, 064107 (2005).
[51] Z. Qian, S. Hou, J. Ning, R. Li, Z. Shen, X. Zhao, and Z. Xue, J. Chem. Phys. **126**, 084705 (2007).
[52] J. F. Kirner, W. Dow, and R. Scheidt, Inorg. Chem. **15**, 1685 (1976).
[53] W. Koch and M. C. Holthausen, *A Chemist's Guide to Density Functional Theory*, 2nd ed. (Wiley, Weinheim, 2001).
[54] N. Marom, O. Hod, G. E. Scuseria, and L. Kronik, J. Chem. Phys. **128**, 164107 (2008).

[55] N. Marom and L. Kronik, Appl. Phys. A: Mater. Sci. Process. **95**, 159 (2009).
[56] N. Marom and L. Kronik, Appl. Phys. A: Mater. Sci. Process. **95**, 165 (2009).
[57] R. Kraus, M. Grobosch, and M. Knupfer, Chem. Phys. Lett. **469**, 121 (2009).
[58] S. Hou, Z. Shen, X. Zhao, and Z. Xue, Chem. Phys. Lett. **373**, 308 (2003).
[59] E. H. Fort, P. M. Donovan, and L. T. Scott, J. Am. Chem. Soc. **131**, 16006 (2009).
[60] S. Banerjee, T. Hemraj-Benny, and S. S. Wong, Adv. Mater. **17**, 17 (2005).
[61] R. Li, S. Hou, J. Zhang, Z. Qian, Z. Shen, and X. Zhao, J. Chem. Phys. **125**, 194113 (2006).